JOC The Journal of Organic Chemistry

Article

pubs.acs.org/joc

The Carbocation Rearrangement Mechanism, Clarified

Daniel J. S. Sandbeck, Daniel J. Markewich, and Allan L. L. East*

Department of Chemistry and Biochemistry, University of Regina, 3737 Wascana Parkway, Regina, SK S4S 0A2, Canada

Supporting Information

ABSTRACT: The role of protonated cyclopropane (PCP^+) structures in carbocation rearrangement is a decades-old topic that continues to confound. Here, quantum-chemical computations (PBE molecular dynamics, PBE and CCSD optimizations, CCSD(T) energies) are used to resolve the issue. PCP^+ intermediates are neither edge-protonated nor corner-protonated (normally) but possess "closed" structures mesomeric between these two. An updated mechanism for hexyl ion rearrangement is presented and shown to resolve past mysteries from isotope-labeling experiments. A new table of elementary-step barrier heights is provided. The mechanism and barrier heights should be useful in understanding and predicting product distributions in organic reactions, including petroleum modification.

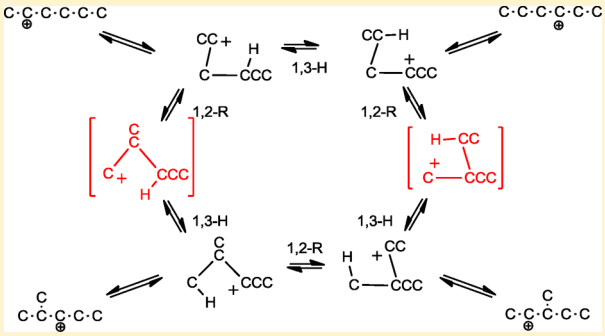

INTRODUCTION

Carbocations are vital intermediates in many organic reactions.[1] In many cases, these intermediates can undergo rapid rearrangement during reaction. There is lingering uncertainty regarding the role and structures of protonated cyclopropane (PCP^+) moieties in rearrangements.[2] Several experimentally known curiosities, including the retardation of alkyl shifts if they result in a different degree of branching,[3,4] remain in want of satisfactory explanation. The confusion, now decades old, is currently adversely affecting attempts to improve kinetic modeling of product distributions in biomass/petroleum refining.[5] This paper clarifies the role and structures of PCP^+ in carbocation rearrangement, supported by a large body of new computational results.

The confusion may be due in part to the continued use of the terms "edge-protonated" and "corner-protonated" to describe PCP^+ intermediates. These terms were used in the 1960s for hypothetical structures.[6] Although such hypothetical structures were used in the earliest semiempirical and ab initio computations on $C_3H_7^+$, once geometry optimization became available it was discovered in 1971 by Radom, Pople, Buss, and Schleyer[7] that the PCP^+ isomer of $C_3H_7^+$ is neither of these (Figure 1) but instead is what they termed a "methyl-eclipsed 1-propyl cation" or a "distorted corner-protonated cyclopropane." In 1939, Wilson suggested that a carbocation intermediate could be "mesomeric" between two classical structures;[8] this "methyl-eclipsed" structure is in a sense even further mesomeric, between the corner-PCP^+ and edge-PCP^+ ideas of the 1960s. We have referred to these meso-PCP^+ alkyl-eclipsed cations as "closed" versions of "open" classical ions for dynamical reasons based on molecular dynamics (MD) simulations.[9]

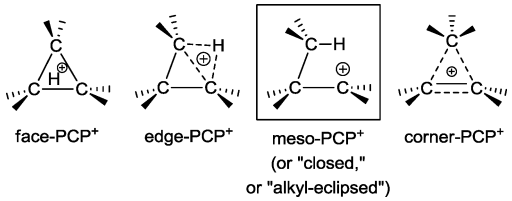

Figure 1. Past hypotheses of PCP^+ intermediate structures. Generally (although exceptions exist) the correct structure is meso-PCP^+.

Radom et al.[7] pointed out that the alkyl-eclipsed structure does not fit well into either the classical or nonclassical ion categories.[2b] This could be one reason why the meso-PCP^+ structure has been underappreciated. The edge-PCP^+ and corner-PCP^+ hypotheses are both decidedly nonclassical, with delocalized three-center–two-electron bond descriptions, but the meso-PCP^+ structure awkwardly benefits from *limited* amounts of *both* of these delocalizations: a hyperconjugative one with a β σ_{CC} bond and neighboring-group participation with a γ σ_{CH} bond. The label of "nonclassical" for PCP^+ structures perhaps became cemented by the Winstein versus Brown dispute over the 2-norbornyl carbocation structure,[10] which regrettably and in hindsight has turned out to be an exception (corner-PCP^+)[11] due to ring strain.[7b] Since meso-PCP^+ does not lend itself to simple three-center–two-electron bond descriptions, we have sketched the structure more "classically" (Figure 1) with the understanding that there is indeed some degree of nonclassical delocalization of electrons.

In 1972, Brouwer and Hogeveen[4] published a review of carbocation rearrangements, summarizing the mechanisms with a complete map of rearrangements for hexyl ion. However, they employed as intermediates the hypothetical edge-PCP^+ and

Received: November 6, 2015
Published: January 26, 2016

ACS Publications © 2016 American Chemical Society

DOI: 10.1021/acs.joc.5b02553
J. Org. Chem. 2016, 81, 1410–1415

corner-PCP$^+$ structures popular at that time. In 1973, Saunders and his group[12] also published a review of carbocation rearrangements, presenting mechanisms employing only corner-PCP$^+$ intermediates. (Saunders et al. referenced the 1971 Radom et al. paper[7a] but seem to have misinterpreted the results as support for corner-PCP$^+$ intermediates.) The 1972 Radom et al. paper[7b] sketched 1,2-methyl- and 1,3-H-shift mechanisms for propyl ion based on the new "alkyl-eclipsed" (meso-PCP$^+$) structure they had found computationally. A perusal of modern texts reveals that confusion still abounds 40 years later and that the outdated terms corner-PCP$^+$ and edge-PCP$^+$ are still in use, albeit cautiously.[2] Since meso-PCP$^+$ structures continued to be found computationally for larger alkyl ions[9,13] we anticipated that mechanisms like those of Radom et al. might generally apply. We thus set upon the tasks of updating the Brouwer–Hogeveen mechanism for hexyl ion rearrangement with the meso-PCP$^+$ ideas of Radom et al. and testing the result with simulations and transition-state computations.[14] The tests were successful. The goal here is to present these results for hexyl ion as a means of clarifying carbocation rearrangement generally, as Brouwer and Hogeveen had first tried to do.

COMPUTATIONAL METHODOLOGY

VASP Simulations. Density functional theory simulations of $C_6H_{13}^+$ were performed using version 5.2.11 of the Vienna Ab Initio Simulation Package (VASP)[15] on the in-house supercomputer Dextrose. The following VASP specifications were used in all of the simulations: potpaw generalized gradient approximation (GGA) plane-wave basis sets,[16,17] standard precision (PREC = Normal), ENMAX = 400 eV, a Nosé thermostat for canonical (*NVT*) conditions[18] with 40 fs thermal oscillations (SMASS = 0), a Verlet velocity algorithm,[19] masses of 12.011 and 1.000 amu for C and H, respectively, and a time step of 1 fs. Since the code cannot turn off its periodic replication algorithm, a single hexyl ion was simulated in a cubic unit cell of width 11 Å together with a homogeneous background negative charge to counterbalance the cation charge (by simply requesting NELECT = 36). Simulations were viewed using Visual Molecular Dynamics (VMD).[20]

Exploratory "rising temperature" runs were initially performed using local density approximation[21,22] forces to gain a feel for what temperatures would be appropriate for viewing which mechanism steps in the limited time windows of an ab initio MD simulation. Then, using Perdew–Burke–Ernzerhof (PBE)[23] forces (GGA = PE), we performed 80 production runs of 20 ps each: 20 at 600 K starting from secondary unbranched ions, 20 at 1000 K starting from the same unbranched ions, 20 at 1000 K starting from secondary monobranched ions, and 20 at 1600 K starting from tertiary ions.

Gaussian Calculations. The Gaussian 03 and Gaussian 09 software packages[24] were used for geometry optimization and higher-accuracy single-point energy calculations of intermediates and transition states. Geometry optimizations used the PBE/6-31G(d,p) and CCSD[25]/6-31G(d,p) levels of theory, the former (requested as PBEPBE/6-31G(d,p)) to mimic as practically as possible the level of theory used in the simulations and the latter to be particularly careful with "hanging-well" minima (common with carbocations), whose existence depends on the level of theory. For transition-state optimizations, we began CCSD searches with HF force constants and ran PBE searches with PBE force constants at every step. From a located transition state, the elementary step was confirmed via minimization geometry optimizations begun from ±-displaced geometries on either side of the transition state. Many conformers were examined.

More accurate single-point energies were computed with the coupled-cluster method CCSD(T)/aug-cc-pVTZ using the PBE/6-31G(d,p) geometries. Thermal corrections (including zero-point vibrational terms) were taken from the PBE/6-31G(d,p) vibrational frequency runs assuming traditional harmonic oscillator/rigid rotor approximations.

RESULTS AND DISCUSSION

The Four Fundamental Steps. With correct incorporation of meso-PCP$^+$ structures, there are four fundamental steps that one should consider for a full rearrangement map for an acyclic carbocation: the 1,2-alkyl and 1,3-H shifts of Radom et al. as well as 1,2-H shifts and internal rotations (Figure 2).

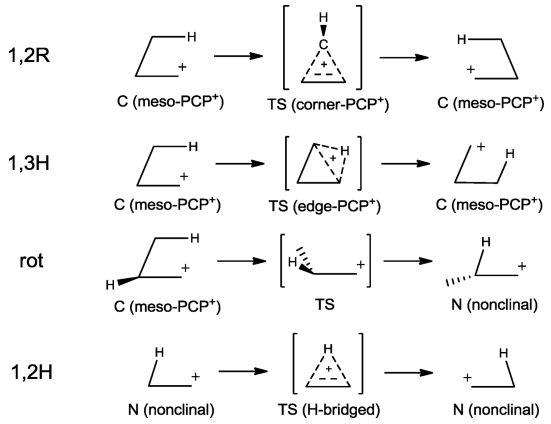

Figure 2. The four fundamental steps in alkyl ion rearrangement. Additional subalkyl groups have been omitted for clarity. These are elementary steps for acyclic secondary carbocations; adjustments to account for primary or tertiary ions will be discussed in terms of these fundamental steps. C and N refer to clinal and nonclinal conformers (see Figure 3).

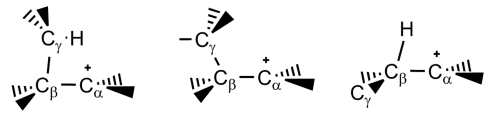

Figure 3. C and N conformers of carbocations.

In Figure 2 we have made use of a distinction between clinal (C) and nonclinal (N) conformers (Figure 3) that we have used before.[9] This language refers to the $\varphi_{(C-C-C^+-C)}$ dihedral angle (~±90° or ~{0°,180°}), which exhibits the internal rotation that allows conversion between these two crucial conformers. An interesting dynamical feature is that the clinal conformer C is "closed" (meso-PCP$^+$) on the potential energy surface (PES) but "open" on the free-energy surface (FES) at sufficiently high temperature.[9b] The internal-rotation step between C and N forms is facile (subpicosecond in 298 K simulations) and for hexyl ion is often not an elementary step on its own. The C/N distinction is useful because 1,2-R shifts and 1,3-H shifts connect clinal structures while 1,2-H shifts connect nonclinal structures.

Correct use of the 1,2-alkyl- and 1,3-H-shift steps allows a correct and satisfying explanation for why branching rearrangements are more inhibited than nonbranching ones. Figure 4 shows a portion of the Brouwer–Hogeveen mechanism[4] and our corrected version. The new mechanism, utilizing the 1,2-methyl and 1,3-H shifts of Radom et al.,[7b] reveals two of the six meso-PCP$^+$ forms to be higher-energy "closed-primary" carbocations (in square brackets) that separate unbranched structures from monobranched ones. This is a general feature of

DOI: 10.1021/acs.joc.5b02553
J. Org. Chem. 2016, 81, 1410–1415

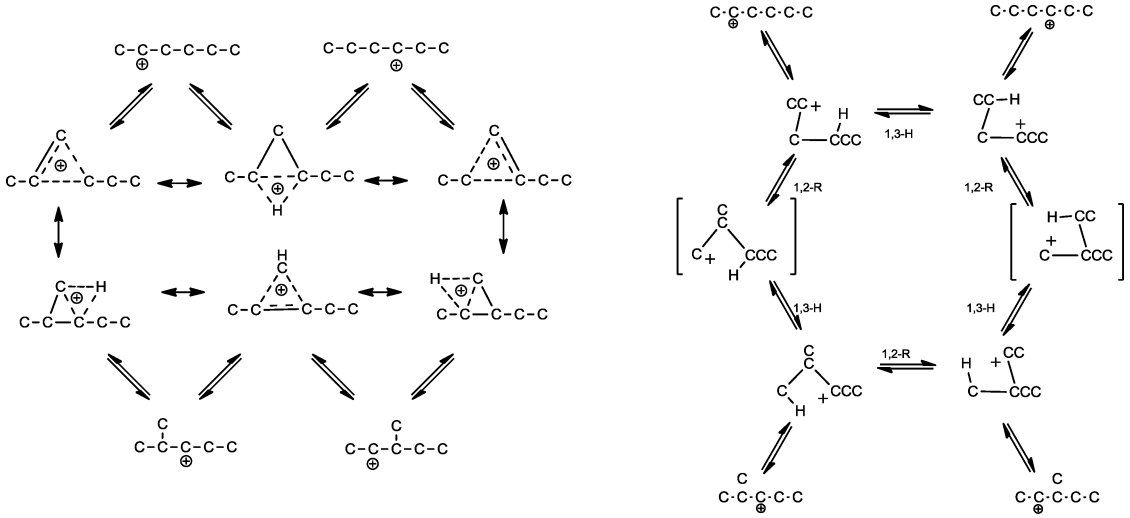

Figure 4. Portion of the incorrect Brouwer–Hogeveen[4] alkyl ion rearrangement mechanism (left) and the updated version (right). Two of the six closed (meso-PCP$^+$) structures in the updated mechanism are closed-primary ions (shown in square brackets). This is the δ cycle in Figure 5.

PCP$^+$ cycles that change the degree of branching. As we will see, these closed-primary structures are transition states here, but when they appear as consecutive structures in other PCP$^+$ cycles, they become nonstationary, separated by a slightly higher-energy transition state.

The Hexyl Ion Rearrangement Map. From these four fundamental steps, the complete hexyl ion rearrangement mechanism is assembled (Figure 5). Each $C_6H_{13}^+$ constitutional isomer **1**–**9** appears in the figure, followed by **C** or **N** to indicate a closed-clinal or nonclinal structure. Since some isomers have two alkyl arms that could "close," the closing arm is indicated by an **A** (larger arm) or **B** (smaller arm). The six PCP$^+$ cycles are labeled α–ζ, and each contains alternating 1,3-H shifts and 1,2-R shifts as in Figure 2. The α cycle interconnects **1**, **3**, **4**, and **7**, while the δ cycle interconnects **5**, **6**, **8**, and **9**; the other four cycles only involve atom scrambling (β for **5**, γ for **2**, ε for **6**, and ζ for **8**). Square brackets (within the α–ζ cycles) and small circles (**1N**, **2N**, and **3N**) denote high-energy (closed-primary) and low-energy (open-tertiary) locations on the PES. The mechanism also includes (i) 1,2-H shifts (**N** to **N** interconversions), (ii) internal rotations about C_α–C_β bonds (**C** to **N** interconversions), and (iii) the only low-energy (secondary-ion-generating) β-scission possible for hexyl ion.

Simulations. The updated mechanism was tested with 80 molecular dynamics simulations of 20 ps each (see the Supporting Information). Runs 1–20, at 600 K starting from unbranched ion **9C** or **8C**, were seen to explore only the unbranched region of Figure 5, having insufficient energy to achieve (in a 20 ps time frame) the closed-primary structure needed for branching. Runs 21–40, at 1000 K starting from the same structures, revealed four instances of branching, all via the δ cycle: three cases of **9C** → **6C** (1,2Pr shift + 1,3H shift) and one case of **8C** → **5C** (1,2Et shift + 1,3H shift). Runs 41–50 (from **5CA**) and 51–60 (from **6CA**), also at 1000 K, rather quickly sank into nearby tertiary carbocation energy wells (**5** → **2** within 2.5 ps and **6** → **3** within 0.5 ps) and did not escape these except in runs 52, 54, and 59; of these, the most adventurous was run 52, which achieved both **5CB** and **5CA** structures and some steps in the β cycle before finishing as tertiary ion **3**. Runs 61–80, at 1600 K starting from **1C** or **3N**, showed some unexpected high-energy β-scission events (due to favorable entropy at this overly high temperature) but also showed several of the steps predicted in Figure 5: the low-energy 1,2alkyl shifts **6CA** → **5CB** (δ cycle) and **5CA** → **5CA** (β cycle), the double 1,2Me shift **1** → **4C** → **1**, the low-energy β-scission from **7**, unbranching **6C** → **9C** (run 74), and, gratifyingly, the full (and experimentally known[26]) *tert* → *tert* **1C** → **3C** conversion, here occurring via 1,2Me, 1,3H, and 1,2Et shifts within a PCP$^+$ structure (run 62). A movie showing this **1C** → **3C** conversion, and another showing the low-energy β scission, are available in the Supporting Information.

Transition-State Optimizations. Seventy different transition states (including conformer variations) were found at the PBE/6-31G(d,p) level, and most were reoptimized at the CCSD/6-31G(d,p) level. They fully support the pathways presented in Figure 5, while revealing the displaced minima and transition states due to the presence of primary and tertiary ions on the map. The 70 different transition-state structures and the energy profiles of the 70 elementary steps are presented in the Supporting Information.

The primary carbocations are indicated in square brackets in Figure 5. Their effect upon elementary steps is as follows. When they appear individually (cycles α and δ) they are transition states, combining a 1,3H and 1,2R pair of fundamental steps into a single ("branching") step. When they appear consecutively (cycles γ, ε, and ζ), they are not stationary points at all: three fundamental steps are combined into a single ("triple-shift") step with a transition state lying between the two primary meso-PCP$^+$ structures (Figure 6).

The tertiary carbocations greatly prefer nonclinal forms (circled in Figure 5). The effect of these nonclinal tertiary ions upon elementary steps is often to turn the neighboring structures listed in Figure 5 into nonstationary shoulders on the potential energy surface, thereby combining two fundamental steps into a single step. For instance, the consecutive internal-rotation and 1,2-H-shift stages for **5CA** → **5N** → **2N** and **6CA** → **6N** → **3N** are combined single steps with a transition state during the internal-rotation stage.

Overall, the results showed relatively consistent barrier heights within a class of step type (see the Supporting Information), and hence, we condensed the results into a table of best results for 16 step classes (Table 1). The relative energies of intermediates can be derived from this table: relative

DOI: 10.1021/acs.joc.5b02553
J. Org. Chem. 2016, 81, 1410–1415

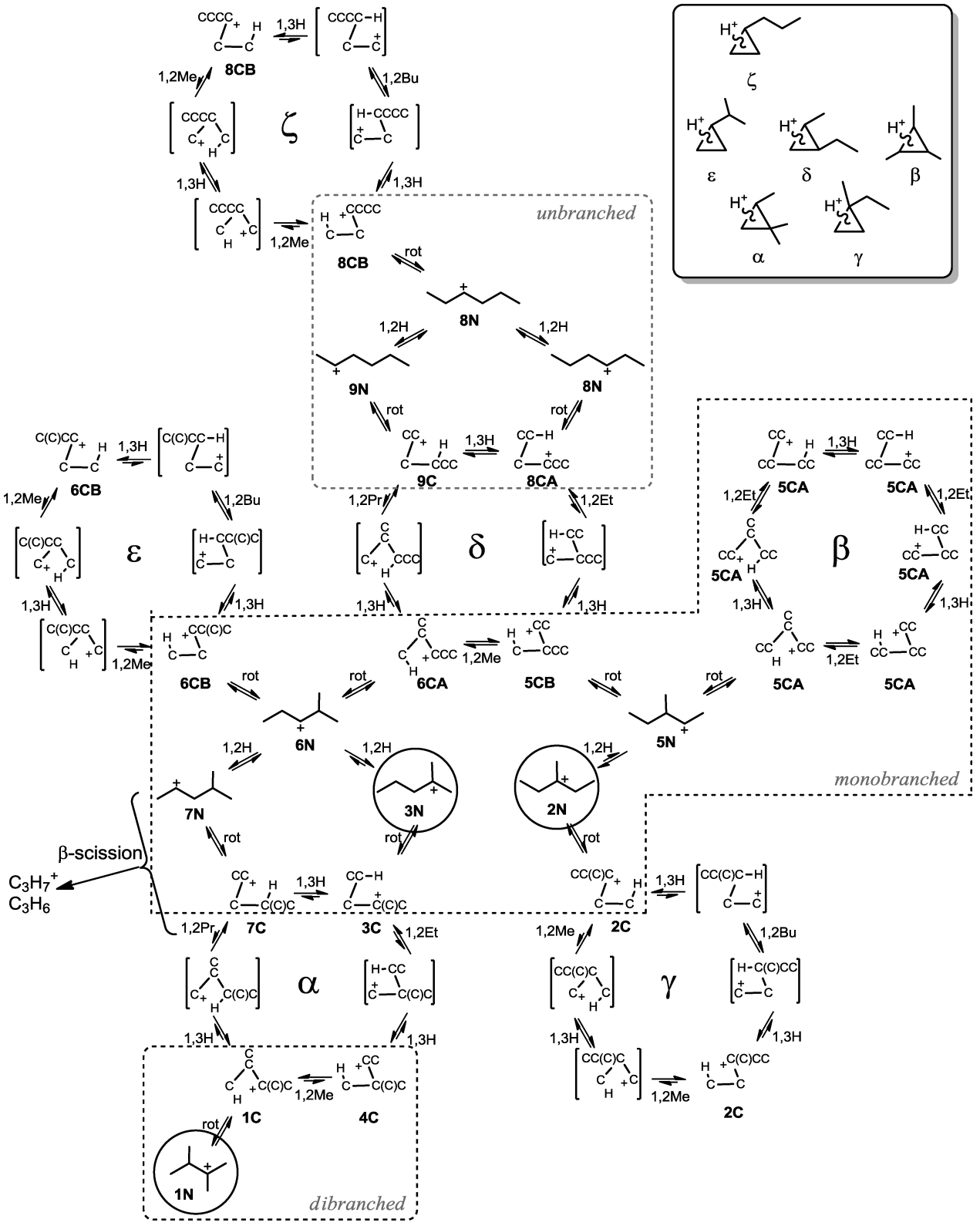

Figure 5. Complete map of hexyl ion rearrangement. Each hexagonal cycle represents interconversion of the six closed (meso) forms of a protonated cyclopropane unit (inset). Notation: **N** = nonclinal, **C** = closed clinal, **CA** = longest arm clinal, **CB** = smallest arm clinal, rot = internal rotation about C_α–C_β bond, [ ] = high-energy closed-primary structure, open circle (**1N**, **2N**, and **3N**) = low-energy open-tertiary intermediate.

to the dibranched tertiary ion **1**, the relative 298 K enthalpies of monobranched tertiary ions (**2** and **3**), monobranched secondary ions (**5**–**7**), and unbranched secondary ions (**8** and **9**) would be 2, 9, and 12 kcal mol^{-1}, respectively. The relative 298 K free energies would be 2, 12, and 13 kcal mol^{-1}, respectively. (Others may wish to fine-tune these results to account for the slightly different energies within each category;

DOI: 10.1021/acs.joc.5b02553
J. Org. Chem. 2016, 81, 1410–1415

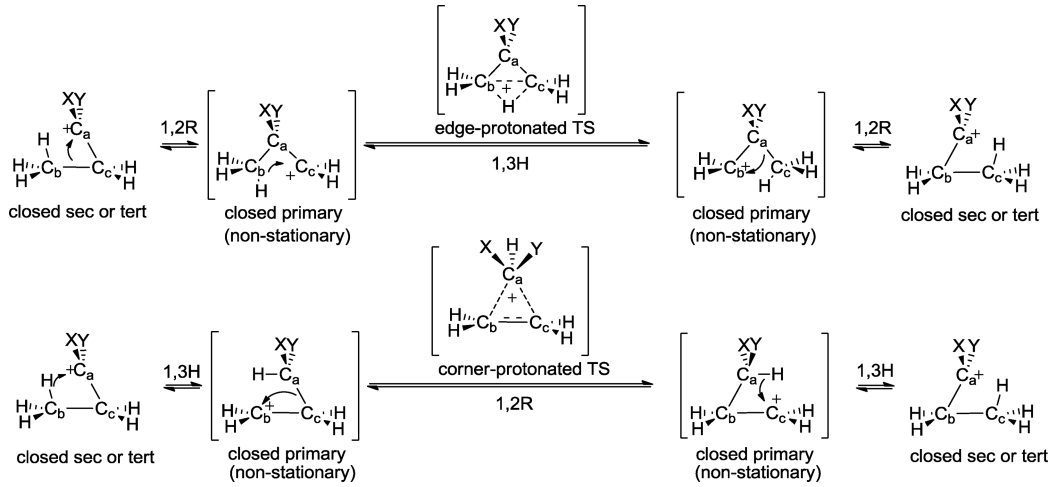

Figure 6. "Triple-shift" steps in the ζ, ε, and γ PCP^+ cycles.

Table 1. Best Estimates of Elementary-Step Barrier Heights for Hexyl Ion Rearrangement (in kcal mol^{-1}) from CCSD(T) Computations

step	$\Delta^{\ddagger}E_{elec}$	$\Delta^{\ddagger}E_0$	$\Delta^{\ddagger}E_{298}$	$\Delta^{\ddagger}H_{298}$	$\Delta^{\ddagger}G_{298}$
1,3H: tert → sec	10	10	9	9	11
1,2H: tert → sec	15	14	14	14	15
branching: tert → tert	15	15	15	15	17
unbranching: tert → tert	17	17	17	17	19
unbranching: tert → sec	18	18	17	17	19
triple shift: tert → tert	20	20	19	19	21
1,2R: sec → sec	0.4	0.2	0	0	1
1,3H: sec → tert	1	1	0	0	1
1,3H: sec → sec	4	3	3	3	4
1,2H: sec → sec	5	4	3	3	4
1,2H: sec → tert	6	5	5	5	5
branching: sec → sec	6	6	5	5	7
branching: sec → tert	7	7	6	6	7
unbranching: sec → sec	9	9	8	8	10
triple shift: sec → sec	14	14	13	13	15
β-scission: sec → sec	37	32	32	33	19

our numbering of isomers **1**–**9** reflects the order of increasing energy in our calculations.)

Discussion. This mechanism resolves many old experimental curiosities. For example: (i) The closed-primary structures account for the rate difference between branching and nonbranching rearrangement.[3,4] (ii) The meso-PCP^+ structure stabilizes closed-secondary ions more than closed-tertiary ones, explaining why 2-butyl carbocation is substantially methyl-bridged[27a] while the 2,3,3-trimethyl-2-butyl carbocation rapidly interconverts between two classical structures.[27b] (iii) Isotope-labeling experiments show more rearrangement in 1-propyl[27c] than in neopentyl[27d,e] because, as in the γ cycle of Figure 5 (left side: 1,2Me shift up to **2C** and then to **2N**), neopentyl has a large thermodynamic drive to form an open-tertiary isopentyl ion rather than to continue around the PCP^+ cycle.

A referee asked whether the proposed mechanism should be restricted to acyclic carbocations. The pathways would not, although ring strain may shift the locations of transition states and intermediates and may effectively block some of the pathways. The aforementioned 2-norbornyl cation features a shift in location of the intermediate from meso-PCP^+ to corner-PCP^+. A second example is the *sec*-cyclohexyl → *tert*-methylcyclopentyl rearrangement; this performs the ringed analogy of the **9N** → **9C** → **6CA** → **6N** → **3N** (or, equivalently, the **8N** → **8C** → **5CB** → **5N** → **2N**) rearrangement with the same crucial closed-primary transition state between **9C** and **6CA**, but features the loss of **9C** as an intermediate because of ring strain.

Finally, we note the relevance to current developments in kinetic modeling of petroleum modification. Klein et al.[5a] hoped to improve the accuracy by reducing the granularity: moving from lumps of molecules (lumped for instance by boiling point range) to molecules themselves. In a 2012 paper,[5b] they made a noble attempt to classify PCP^+-related isomerizations for this purpose, but because of the lack of precise knowledge of PCP^+ mechanisms, they proposed a classification that will not be effective. They in effect assumed that the classification used by Weitkamp et al.[28] for β-scission would work for rearrangement: A for *tert* → *tert*, B1 for *sec* → *tert*, B2 for *tert* → *sec*, and C for *sec* → *sec*. It will not. First, this lacks the separation of slower branching steps from faster nonbranching steps; for instance, their C examples #1 to #4 (branching, in the PCP^+ α cycle) should be in a different class from their C examples #5 to #8 (nonbranching, in the PCP^+ β cycle). Second, considering branching steps alone, the rates of these four classes A/B1/B2/C *do not appreciably differ*, with barriers of 17–19 kcal mol^{-1} above the PES global minimum. Weitkamp's classifications for β-scission were based on clear distinctions in rate. We offer Table 1 in the hopes that this can lead to improved classifications for such modeling.

In closing, the true role of PCP^+ is as a meso-PCP^+ structure that as an intermediate effects facile 1,2R and 1,3H shifts and as a transition state effects traversable branching steps.

■ ASSOCIATED CONTENT

Supporting Information

The Supporting Information is available free of charge on the ACS Publications website at DOI: 10.1021/acs.joc.5b02553.

Movie 1 showing the triple-shift **1** → **3** isomerization in run 62 (MPG)

Movie 2 showing the sequence **3** → **7** → β-scission later in run 62 (MPG)

Computational methods, summaries of 80 simulations and transition-state studies, Gaussian logfile energies, and

DOI: 10.1021/acs.joc.5b02553
J. Org. Chem. 2016, 81, 1410–1415

Cartesian coordinates of the 70 PBE/6-31G(d,p) transition states (PDF)

AUTHOR INFORMATION

Corresponding Author

*E-mail: allan.east@uregina.ca.

Notes

The authors declare no competing financial interest.

ACKNOWLEDGMENTS

We gratefully acknowledge NSERC (Canada) for operational grant funding and the Canada Foundation for Innovation, the Government of Saskatchewan, and CiaraTech (Canada) for supercomputer funding. The Laboratory of Computational Discovery (John Jorgensen and Robert Cowles, sysadmins) is thanked for supercomputer upkeep. A. M. Wagaye (Ethiopia) is thanked for initial exploratory calculations.[14]

REFERENCES

(1) Naredla, R. R.; Klumpp, D. A. *Chem. Rev.* **2013**, *113*, 6905.

(2) (a) Smith, M. B. *March's Advanced Organic Chemistry*, 7th ed.; Wiley: Hoboken, NJ, 2013; pp 1526−7. (b) Olah, G. A.; Surya Prakash, G. K.; Molnár, A.; Sommer, J. *Superacid Chemistry*, 2nd ed.; Wiley: Hoboken, NJ, 2009; p 527.

(3) (a) Brouwer, D. M. *Recl. Trav. Chim. Pays Bas* **1968**, *87*, 210. (b) Brouwer, D. M.; Oelderik, J. M. *Recl. Trav. Chim. Pays Bas* **1968**, *87*, 721.

(4) Brouwer, D. M.; Hogeveen, H. *Prog. Phys. Org. Chem.* **1972**, *9*, 179.

(5) (a) Klein, M. T.; Hou, G.; Bertolacini, R. J.; Broadbelt, L. J.; Kumar, A. *Molecular Modeling in Heavy Hydrocarbon Conversions*, 1st ed.; CRC Press: Boca Raton, FL, 2006. (b) Bennett, C. A.; Klein, M. T. *Energy Fuels* **2012**, *26*, 41.

(6) Collins, C. J. *Chem. Rev.* **1969**, *69*, 543.

(7) (a) Radom, L.; Pople, J. A.; Buss, V.; Schleyer, P. v. R. *J. Am. Chem. Soc.* **1971**, *93*, 1813;(b) *J. Am. Chem. Soc.* **1972**, *94*, 311.

(8) Nevell, T. P.; de Salas, E.; Wilson, C. L. *J. Chem. Soc.* **1939**, 1188.

(9) (a) East, A. L. L.; Bučko, T.; Hafner, J. *J. Phys. Chem. A* **2007**, *111*, 5945. (b) East, A. L. L.; Bučko, T.; Hafner, J. *J. Chem. Phys.* **2009**, *131*, 104314.

(10) Olah, G. A. *J. Org. Chem.* **2001**, *66*, 5943.

(11) (a) Olah, G. A.; White, A. M. *J. Am. Chem. Soc.* **1969**, *91*, 3954. (b) Olah, G. A.; White, A. M. *J. Am. Chem. Soc.* **1969**, *91*, 3956. (c) Yannoni, C. S.; Macho, V.; Myhre, P. C. *J. Am. Chem. Soc.* **1982**, *104*, 7380. (d) Scholz, F.; Himmel, D.; Heinemann, F. W.; Schleyer, P. v. R.; Meyer, K.; Krossing, I. *Science* **2013**, *341*, 62.

(12) Saunders, M.; Vogel, P.; Hagen, E. L.; Rosenfeld, J. *Acc. Chem. Res.* **1973**, *6*, 53.

(13) (a) Carneiro, J. W. de M.; Schleyer, P. v. R.; Koch, W.; Raghavachari, K. *J. Am. Chem. Soc.* **1990**, *112*, 4064. (b) Sieber, S.; Buzek, P.; Schleyer, P. v. R.; Koch, W.; Carneiro, J. W. de M. *J. Am. Chem. Soc.* **1993**, *115*, 259.

(14) Results from preliminary LDA and QCISD calculations, and the improved mechanism presented here (due to A. East), first appeared in a thesis of an East group student (see: Wagaye, A. M. M.Sc. Thesis, University of Regina, Regina, SK, 2011).

(15) (a) Kresse, G.; Hafner, J. *Phys. Rev. B: Condens. Matter Mater. Phys.* **1993**, *47*, 558. (b) Kresse, G.; Furthmüller, J. *Phys. Rev. B: Condens. Matter Mater. Phys.* **1996**, *54*, 11169.

(16) Kresse, G.; Hafner, J. *J. Phys.: Condens. Matter* **1994**, *6*, 8245.

(17) Kresse, G.; Joubert, D. *Phys. Rev. B: Condens. Matter Mater. Phys.* **1999**, *59*, 1758.

(18) Nosé, S. A. *J. Chem. Phys.* **1984**, *81*, 511.

(19) Leach, A. R. *Molecular Modelling: Principles and Applications*, 2nd ed.; Pearson Education Ltd.: Harlow, U.K., 2001.

(20) Humphrey, W.; Dalke, A.; Schulten, K. *J. Mol. Graphics* **1996**, *14*, 33.

(21) Perdew, J. P.; Zunger, A. *Phys. Rev. B: Condens. Matter Mater. Phys.* **1981**, *23*, 5048.

(22) Vosko, S. H.; Wilk, L.; Nusair, M. *Can. J. Phys.* **1980**, *58*, 1200.

(23) (a) Perdew, J. P.; Burke, K.; Ernzerhof, M. *Phys. Rev. Lett.* **1996**, *77*, 3865;(b) *Phys. Rev. Lett.* **1997**, *78*, 1396.

(24) Frisch, M. J.; et al. *Gaussian 09*, revision B.01; Gaussian, Inc.: Wallingford, CT, 2010.

(25) Scuseria, G. E.; Janssen, C. L.; Schaefer, H. F., III *J. Chem. Phys.* **1988**, *89*, 7382.

(26) Olah, G. A.; Lukas, J. *J. Am. Chem. Soc.* **1967**, *89*, 4739.

(27) (a) Johnson, S. A.; Clark, D. T. *J. Am. Chem. Soc.* **1988**, *110*, 4112. (b) Olah, G. A.; DeMember, J. R.; Commeyras, A.; Bribes, J. L. *J. Am. Chem. Soc.* **1971**, *93*, 459. (c) Karabatsos, G. J.; Orzech, C. E., Jr.; Fry, J. L.; Meyerson, S. *J. Am. Chem. Soc.* **1970**, *92*, 606. (d) Skell, P. S.; Starer, I.; Krapcho, A. P. *J. Am. Chem. Soc.* **1960**, *82*, 5257. (e) Karabatsos, G. J.; Orzech, C. E., Jr.; Meyerson, S. *J. Am. Chem. Soc.* **1964**, *86*, 1994.

(28) Weitkamp, J.; Jacobs, P. A.; Martens, J. A. *Appl. Catal.* **1983**, *8*, 123.

DOI: 10.1021/acs.joc.5b02553
J. Org. Chem. 2016, 81, 1410−1415